Available online at www.eccomasproceedia.org
Eccomas Proceedia COMPDYN (2017) 2937-2949

ECCOMAS
Proceedia

COMPDYN 2017
6th ECCOMAS Thematic Conference on
Computational Methods in Structural Dynamics and Earthquake Engineering
M. Papadrakakis, M. Fragiadakis (eds.)
Rhodes Island, Greece, 15–17 June, 2017

A NEW COMPUTATIONAL APPROACH FOR THE ROCKING RESPONSE OF DEFORMABLE BODIES CONSIDERING MATERIAL NONLINEARITY

Evangelos Avgenakis and Ioannis N. Psycharis

School of Civil Engineering
National Technical University of Athens, Greece
Polytechnic Campus, Heroon Polytechniou 9, 15780 Zografou
e-mail: vavgen@outlook.com, ipsych@central.ntua.gr

Keywords: Rocking, Macroelement, Nonlinear analysis, Inelastic response, Resilient structures.

Abstract. *An increasing interest in the use of rocking members in earthquake resistant structural systems has been observed in recent years. The benefits of such members include the limitation of the damage, re-centering capabilities and reduction of seismic forces transmitted to the rest of the structure due to a yield-like response.*

Despite the importance of such members, few models able to describe the response of flexible rocking members in structural systems realistically can be found in literature, since most of the research focuses on the response of rigid bodies or ignores the stress nonlinearity near the contact area, which is considered crucial to the accurate determination of the rocking response of deformable rocking bodies. A new macro-element formulation for elastic rocking members has been proposed by the authors in previous papers which is able to take into account this stress nonlinearity, producing results which are very close to the ones produced by conventional finite element programs.

Rocking members in structural systems are expected to behave inelastically for large seismic excitations. In this paper, the macroelement presented previously by the authors, which considered the element material to be elastic, is extended to also take material nonlinearity into account. The effect of the nonlinear stress distribution across the rocking interface on the member displacements is determined and approximate formulas for their determination are included in the macro-element formulation. The results produced by the macro-element with the inelastic material are finally compared to the ones of conventional finite element codes, showing very good agreement between the results of the two methods.

Peer-review under responsibility of the organizing committee of COMPDYN 2017.
doi: 10.7712/120117.5618.17884

1 INTRODUCTION

The rocking motion of rigid bodies and structural members has recently gained an increased attention from the scientific community. Unlike members considered in classical mechanics, which can transmit tensile stresses through their base, members unrestrained or partially restrained at their base can develop only compressive stresses, while uplift occurs, altering significantly their response. When large enough horizontal forces are imposed on the member, its base partially detaches from the ground and the body rotates about one of its corners. The vertical force acts as the restoring force that tends to bring the body back to its original equilibrium position.

The inclusion of rocking members in real structures is considered a promising solution to the design of resilient structures. During a seismic event, conventional structural elements are designed to gradually yield and develop damage and residual deformations, requiring repairs afterwards. In contrast, rocking members exhibit a yield-like response, able to limit the forces transmitted to the structure during an earthquake, developing however little damage and residual deformations.

Up to date, rocking members have been applied in case of bridge piers (e.g. the Rangitikei Railway Bridge [1]), while extensive analytical and experimental work has been performed on rocking shear walls in precast structures (e.g. [2], [3], [4]). Furthermore, guidelines addressing this alternative seismic design have been published by several organizations.

Various analytic solutions exist regarding the motion of the rigid rocking block (e.g. [5], [6], [7], [8]), as well as approximate formulas for the design of controlled rocking systems. However, few computational models exist for modeling the response of deformable rocking bodies (e.g. [9], [10], [11], [12], [13], [14], [15], [16], [17]). Most of these studies, though, consider the rocking base to be rigid, take into account the stress nonlinearity only across the rocking interface or make simplifications regarding the stress distribution near the contact area.

A new macroelement formulation has been recently proposed by the authors ([18]), which is able to take into account both the deformability of the rocking member along its height, as well as the stress nonlinearity near the contact area, which is crucial in many applications, especially regarding members with constrained rocking motion. The material in this macroelement was assumed to be elastic. However, rocking members in structural systems are expected to behave inelastically for large seismic excitations. So, in this paper, the previous formulation is extended to also take material nonlinearity into account for monotonic loading.

2 ELASTIC MATERIAL FORMULATION

The basic steps of the elastic material formulation found in [18] are summarized here, since this also serves as the basis of the material nonlinearity formulation.

First of all, the member is examined in a natural coordinate system without rigid body modes. This coordinate system corresponds to a coordinate system of a simply supported beam along the deformed position of the member and has three independent degrees of freedom, $\bar{\boldsymbol{q}}$. For space reasons, the conversion between the local and the natural coordinate system is not repeated here, but can be found in the original paper.

Given the natural system displacements and the corresponding displacement increments, a vector of natural system nodal forces, $\bar{\boldsymbol{Q}}$, is estimated using the existing stiffness matrix. From these forces, a vector of displacements according to the techical theory of bending can be calculated, as in conventional finite elements.

However, since these forces do not act on the whole rocking interface, as only compressive

stresses are allowed to develop, the stress distributions at the contact surface differ from those of the technical theory of bending and produce nonlinear stress distributions near the contact area. In order to account for the difference between the stresses assumed by the technical theory and the real ones, self-equilibrating stresses at the rocking interface are considered, which influence the local deformations and give rise to additional displacements. The influence of these self-equilibrating stresses is examined by considering the equivalent problem of a semi-infinite strip loaded with self-equilibrating stresses on its free side [19].

For a given natural system force vector, $\bar{\boldsymbol{Q}}$, the forces at the rocking end, $\bar{\boldsymbol{Q}}_{\mathrm{r}} = [N_{\mathrm{r}}, M_{\mathrm{r}}, Q_{\mathrm{r}}]^{\mathrm{T}}$, for a member with length L, normalized with respect to the member thickness, W, are given by

$$\bar{\boldsymbol{Q}}_{\mathrm{r}} = \boldsymbol{S}_1 \, \bar{\boldsymbol{Q}} \tag{1}$$

where

$$\boldsymbol{S}_1 = \frac{1}{W} \begin{bmatrix} 1 & 0 & 0 \\ 0 & 1 & 0 \\ 0 & -\dfrac{1}{L} & -\dfrac{1}{L} \end{bmatrix} \tag{2}$$

Assuming a triangular normal and a parabolic shear stress distribution at the rocking interface, the normalized stress distribution parameter vector, $\boldsymbol{r} = [c, \widetilde{\sigma}_{\mathrm{m}}, \widetilde{\tau}_{\mathrm{m}}]^T$, correspoding to the normalized contact length, the maximum normal and the maximum shear stress of a member with semiwidth $b = 1$, is calculated:

$$\boldsymbol{r} = \begin{Bmatrix} 3\left(1 + \dfrac{\rho M_{\mathrm{r}}}{b N_{\mathrm{r}}}\right) \\ \dfrac{2}{3} \dfrac{N_{\mathrm{r}}}{b + \frac{\rho M_{\mathrm{r}}}{N_{\mathrm{r}}}} \\ \dfrac{1}{2} \dfrac{\rho Q_{\mathrm{r}}}{b + \frac{\rho M_{\mathrm{r}}}{N_{\mathrm{r}}}} \end{Bmatrix} \tag{3}$$

where ρ is the signum function of M_{r} and b is the semiwidth of the original member.

The additional displacements due to the self-equilibrating stresses can be evaluated by approximating the fiber elongation profile across the loaded area of the rocking interface using a linear distribution, whose parameters correspond to the axial elongation at the center of the section and the rotation of the rocking end. Using the load parameter vector, $\boldsymbol{r}$, these additional displacements can be estimated from

$$\boldsymbol{u} = \frac{1}{E} \begin{Bmatrix} \left(\widetilde{\sigma}_{\mathrm{m}} \, \boldsymbol{V}_{\sigma}^{\mathrm{T}} + \widetilde{\tau}_{\mathrm{m}} \, \boldsymbol{V}_{\tau}^{\mathrm{T}}\right) \boldsymbol{P}_c \\ \left(\widetilde{\sigma}_{\mathrm{m}} \, \boldsymbol{R}_{\sigma}^{\mathrm{T}} + \widetilde{\tau}_{\mathrm{m}} \, \boldsymbol{R}_{\tau}^{\mathrm{T}}\right) \boldsymbol{P}_c \end{Bmatrix} \tag{4}$$

in which

$$\boldsymbol{P}_c = \begin{bmatrix} c^6 & c^5 & c^4 & c^3 & c^2 & c & 1 \end{bmatrix}^T \tag{5}$$

$$\begin{aligned} \boldsymbol{V}_{\tau} &= \boldsymbol{V}_{\tau 0} + \nu \boldsymbol{V}_{\tau \nu} \\ \boldsymbol{R}_{\tau} &= \boldsymbol{R}_{\tau 0} + \nu \boldsymbol{R}_{\tau \nu} \end{aligned} \tag{6}$$

and the polynomial constant term $\boldsymbol{V}_{\sigma}$ and $\boldsymbol{R}_{\sigma}$ (for the normal stress contribution) and $\boldsymbol{V}_{\tau 0}$, $\boldsymbol{V}_{\tau \nu}$, $\boldsymbol{R}_{\tau 0}$, $\boldsymbol{R}_{\tau \nu}$ (for the shear stress contribution) vectors given in [18].

Thus, the displacements due to the self-equilibrating stresses in the original member natural coordinate system are:

$$\bar{\boldsymbol{q}}_{\text{se}} = \boldsymbol{S}_3\, \boldsymbol{u} \tag{7}$$

where

$$\boldsymbol{S}_3 = \begin{bmatrix} b & 0 \\ 0 & \rho \\ 0 & 0 \end{bmatrix} \tag{8}$$

The corresponding flexibility matrix of the self-equilibrating stresses contribution is

$$\bar{\boldsymbol{F}}_{\text{se}} = \frac{\partial \bar{\boldsymbol{q}}_{\text{se}}}{\partial \bar{\boldsymbol{Q}}} = \boldsymbol{S}_3\, \bar{\boldsymbol{F}}_n\, \boldsymbol{S}_2\, \boldsymbol{S}_1 \tag{9}$$

where

$$\boldsymbol{S}_2 = \frac{\partial \boldsymbol{r}}{\partial \bar{\boldsymbol{Q}}_{\text{r}}} = \begin{bmatrix} \dfrac{6-2c}{bc\widetilde{\sigma}_{\text{m}}} & \dfrac{6\rho}{b^2 c\widetilde{\sigma}_{\text{m}}} & 0 \\ \dfrac{4c-6}{bc^2} & -\dfrac{6\rho}{b^2c^2} & 0 \\ \dfrac{2\widetilde{\tau}_{\text{m}}(c-3)}{bc^2\widetilde{\sigma}_{\text{m}}} & -\dfrac{6\rho\widetilde{\tau}_{\text{m}}}{b^2c^2\widetilde{\sigma}_{\text{m}}} & \dfrac{3\rho}{2bc} \end{bmatrix} \tag{10}$$

and

$$\bar{\boldsymbol{F}}_n = \frac{1}{E} \begin{bmatrix} \left(\widetilde{\sigma}_{\text{m}}\, \boldsymbol{V}_\sigma^{\text{T}} + \widetilde{\tau}_{\text{m}}\, \boldsymbol{V}_\tau^{\text{T}}\right) \boldsymbol{P}_c' & \boldsymbol{V}_\sigma^{\text{T}}\, \boldsymbol{P}_c & \boldsymbol{V}_\tau^{\text{T}}\, \boldsymbol{P}_c \\ \left(\widetilde{\sigma}_{\text{m}}\, \boldsymbol{R}_\sigma^{\text{T}} + \widetilde{\tau}_{\text{m}}\, \boldsymbol{R}_\tau^{\text{T}}\right) \boldsymbol{P}_c' & \boldsymbol{R}_\sigma^{\text{T}}\, \boldsymbol{P}_c & \boldsymbol{R}_\tau^{\text{T}}\, \boldsymbol{P}_c \end{bmatrix} \tag{11}$$

with

$$\boldsymbol{P}_c' = \begin{bmatrix} 6c^5 & 5c^4 & 4c^3 & 3c^2 & 2c & 1 & 0 \end{bmatrix}^T \tag{12}$$

The displacements and the flexibility matrix of the self-equilibrating stresses contribution are finally added to those of the technical theory of bending. Since these natural system displacements generally differ from the ones assumed in the beginning, their difference is multiplied with the total flexibility matrix and this additional term is added to the nodal forces assumed. If this term is large enough, an iteration of the procedure is performed.

3 EXTENSION TO THE INELASTIC MATERIAL CASE

For the solution of the inelastic material case, new stress distributions acting on the rocking interface have to be assumed. As a simplification, the area inside the element is considered to behave elastically, so that the existing solution of the semi-infinite strip stress problem, based on the theory of elasticity, as well as the principle of superposition hold. However, as discussed in the ensuing, this assumption does not lead to results far from the reality, since only the elongations of the elastic portion of the section are taken into account.

For the normal stresses, a trapezoidal stress distribution is assumed to act on the rocking interface, after yielding occurs (Fig. 1). In order to examine the response of the member under the trapezoidal loading, a new parameter μ can be defined:

$$\mu = \frac{c_y}{c} \tag{13}$$

where c_y is the length of the contact area which has yielded.

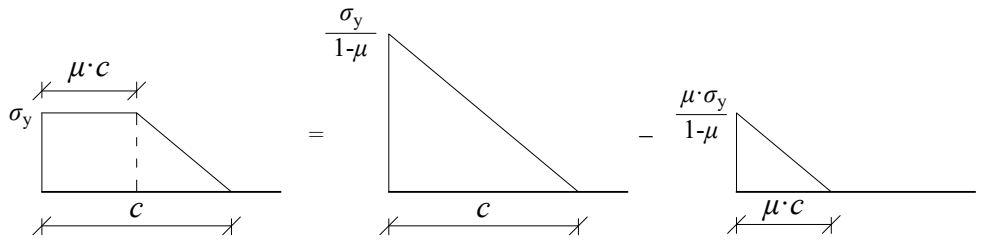

Figure 1: Normal stress distribution acting on the rocking interface after yielding and decomposition into triangular distributions.

The resultant axial force and moment can be expressed as:

$$N_{\mathrm{r}} = \frac{1}{2}(1+\mu)bc\sigma_y \tag{14}$$

$$M_{\mathrm{r}} = \rho\left[\frac{1}{2}(1+\mu)b^2c\left(\frac{c}{3}-1\right)\sigma_y + \frac{1}{6}\mu^2b^2c^2\sigma_y\right] \tag{15}$$

where ρ is the signum function of M.

The trapezoidal distribution can be expressed as the difference of the two triangular distributions with parameters ($\sigma_y/(1-\mu)$,c) and ($\mu\sigma_y/(1-\mu)$,μc) shown in Fig. 1. Assuming that the shear stress distribution results from the difference of two parabolic distributions corresponding to the aforementioned triangular normal stress distributions and that the ratio of the maximum shear stress values is the same as the maximum normal stresses ratio, the resultant shear force is

$$Q_{\mathrm{r}} = \rho\frac{2}{3}(1-\mu^2)bct \tag{16}$$

where t is the maximum shear stress corresponding to the distribution of contact length c.

Given a vector of resultant forces acting on the rocking interface, $\bar{\boldsymbol{Q}}_{\mathrm{r}}$, the load distribution parameter vector, $\boldsymbol{r}_{\mathrm{y}} = [c, \mu, t]^T$, can be calculated from:

$$\boldsymbol{r}_{\mathrm{y}} = \begin{Bmatrix} c \\ \mu \\ t \end{Bmatrix} = \begin{Bmatrix} \dfrac{N_{\mathrm{r}}\omega}{\sigma_{\mathrm{y}}b} \\ \dfrac{2}{\omega} - 1 \\ \dfrac{3\rho\omega^2 Q_{\mathrm{r}}}{8(\omega-1)bc} \end{Bmatrix} \tag{17}$$

where

$$\omega = \sqrt{3\left(\frac{2b\sigma_{\mathrm{y}}}{N_{\mathrm{r}}} + \frac{2\rho M_{\mathrm{r}}\sigma_{\mathrm{y}}}{N_{\mathrm{r}}^2} - 1\right)} + 1 \tag{18}$$

The corresponding derivative matrix of the load parameters to the rocking end forces is

$$\boldsymbol{S}_{2\mathrm{y}} = \frac{\partial \boldsymbol{r}_{\mathrm{y}}}{\partial \bar{\boldsymbol{Q}}_{\mathrm{r}}} = \begin{bmatrix} \dfrac{2(c+2\mu c-3)}{(\mu-1)bc\sigma_{\mathrm{y}}} & -\dfrac{6\rho}{(\mu-1)b^2c\sigma_{\mathrm{y}}} & 0 \\ \dfrac{6(\mu+1)-4(1+\mu+\mu^2)c}{(\mu-1)bc^2\sigma_{\mathrm{y}}} & \dfrac{6\rho(\mu+1)}{(\mu-1)b^2c^2\sigma_{\mathrm{y}}} & 0 \\ \dfrac{2ct(2\mu^3+3\mu^2+6\mu+1)-6t(1+\mu)^2}{(\mu-1)^2(\mu+1)bc^2\sigma_{\mathrm{y}}} & -\dfrac{6\rho t(\mu+1)}{(\mu-1)^2b^2c^2\sigma_{\mathrm{y}}} & \dfrac{3\rho}{2bc(1-\mu^2)} \end{bmatrix} \tag{19}$$

It is noted that the material yields when

$$\sigma_{\mathrm{y}} > \frac{2N_{\mathrm{r}}}{3\left(b + \frac{\rho M_{\mathrm{r}}}{N_{\mathrm{r}}}\right)} \tag{20}$$

4 ADDITIONAL DISPLACEMENTS DUE TO THE SELF-EQUILIBRATING STRESSES

As for the elastic material case, the self-equilibrating stress distributions originating from the aforementioned ones are examined using the semi-infinite strip problem solution. However, the additional displacements due to these self equilibrating stresses are not calculated by approximation of the whole contact area fiber elongation profile with a linear distribution, but only of the portion of the section that remains elastic, that is in the interval $[-1+\mu c, -1+c]$. This can be applied, since the fibers under this area are assumed to remain elastic, in contrast to the fibers under the yielded contact zone.

Using the aforementioned procedure, the self-equilibrating stresses normalized displacement approximation formula presented next is produced, giving very good results for $c \leq 2/(\mu+1)$, which includes most of the usual cases:

$$\boldsymbol{u}_y = \frac{1}{E}\begin{Bmatrix}\sigma_{\mathrm{y}}\delta_\sigma(c,\mu) + t\delta_\tau(c,\mu)\\ \sigma_{\mathrm{y}}\theta_\sigma(c,\mu) + t\theta_\tau(c,\mu)\end{Bmatrix} \tag{21}$$

where the functions $\delta_\sigma(c,\mu), \theta_\sigma(c,\mu), \delta_t(c,\mu), \theta_t(c,\mu)$ are presented in the following.

Normal stresses Introducing a normalized contact length $c_{\mathrm{n}} = c(\mu+1)$, functions $\delta_\sigma(c,\mu)$ and $\theta_\sigma(c,\mu)$ are given by:

$$\delta_\sigma = \delta_A(c_{\mathrm{n}}) + \delta_B(\mu)(c_{\mathrm{n}} - 2) \tag{22}$$
$$\theta_\sigma = \theta_A(c_{\mathrm{n}}) + \theta_B(\mu) + \theta_C(\mu)\theta_D(c_{\mathrm{n}}) \tag{23}$$

where the various functions appearing in these equations have the forms:

$$\delta_A(c_{\mathrm{n}}) = a_1\left[1 - (c_{\mathrm{n}}/2)^{a_2}\right]^{a_3} \tag{24}$$
$$\delta_B(\mu) = a_1\tan(a_2\mu) + a_3\mu + a_4\mu^2 + a_5\mu^3 \tag{25}$$
$$\theta_A(c_{\mathrm{n}}) = a_1\left[1 - (c_{\mathrm{n}}/2)^{a_2}\right]^{a_3}(1 - c_{\mathrm{n}}/2)^2 \tag{26}$$
$$\theta_B(\mu) = a_1\tan(a_2\mu) + a_3\mu + a_4\mu^2 + a_5\mu^3 \tag{27}$$
$$\delta_C(\mu) = a_1\mu^4 + a_2\mu^3 + a_3\mu^2 + (-4a_1 - 3a_2 - 2a_3)\mu \tag{28}$$
$$\delta_D(c_{\mathrm{n}}) = a_1 c_{\mathrm{n}}^6 + a_2 c_{\mathrm{n}}^5 + a_3 c_{\mathrm{n}}^4 + a_4 c_{\mathrm{n}}^3 + (-16a_1 - 8a_2 - 4a_3 - 2a_4 + 0.25)c_{\mathrm{n}}^2 \tag{29}$$

The constant parameters appearing in these equations are given in Table 1.

Furthermore, the following derivatives are calculated, which are needed in the following:

$$\frac{\partial\delta_\sigma}{\partial c} = (\mu+1)\left(\frac{d\delta_A}{dc_{\mathrm{n}}} + \delta_B\right) \tag{30}$$
$$\frac{\partial\delta_\sigma}{\partial \mu} = c\left(\frac{d\delta_A}{dc_{\mathrm{n}}} + \delta_B\right) + \frac{d\delta_B}{d\mu}(c_{\mathrm{n}} - 2) \tag{31}$$
$$\frac{\partial\theta_\sigma}{\partial c} = (\mu+1)\left(\frac{d\theta_A}{dc_{\mathrm{n}}} + \theta_C\frac{d\theta_D}{dc_{\mathrm{n}}}\right) \tag{32}$$
$$\frac{\partial\theta_\sigma}{\partial \mu} = c\left(\frac{d\theta_A}{dc_{\mathrm{n}}} + \theta_C\frac{d\theta_D}{dc_{\mathrm{n}}}\right) + \frac{d\theta_B}{d\mu} + \theta_D\frac{d\theta_C}{d\mu} \tag{33}$$

Table 1: Approximation functions constant term vectors

Function	a_1	a_2	a_3	a_4
δ_A	-1.61868182	0.74341712	2.38990044	
δ_B	0.02707282	0.71805567	-0.42532673	0.64748945
θ_A	-1.60601045	2.71616773	0.52133449	
θ_B	-0.05393963	-1.54431579	0.98577157	-1.35812515
θ_C	-0.4009598	1.46727493	-2.19487061	
θ_D	-0.03040586	0.15378978	-0.33644138	0.38440043
δ_1	2.48001601	0.68431159	1.80867566	
δ_2	-0.43362038			
θ_1	2.35842517	0.98635297	1.52894546	
θ_2	-0.45228844			

It is noted that for $c > 2/(\mu + 1)$, due to the symmetry of the self-equilibrating normal stresses, the following equations hold:

$$\delta_\sigma(c, \mu) = -\delta_\sigma(2 - \mu c, (2 - c)/(2 - \mu c)) \tag{34}$$
$$\theta_\sigma(c, \mu) = \theta_\sigma(2 - \mu c, (2 - c)/(2 - \mu c)) \tag{35}$$

A comparison between the semi-infinite strip problem results and the ones predicted from the aforementioned equations can be seen in Fig. 2.

Shear stresses

$$\delta_\tau = \delta_1(c)\delta_2(\mu) \tag{36}$$
$$\theta_\tau = \theta_1(c)\theta_2(\mu) \tag{37}$$

where the functions appearing in these equations have the forms:

$$\delta_1(c) = a_1 \left[1 - (c/2)^{a_2}\right]^{a_3} \tag{38}$$
$$\delta_2(\mu) = (a_1\mu - 1)(\mu - 1) \tag{39}$$
$$\theta_1(c) = a_1 \left[1 - (c/2)^{a_2}\right]^{a_3} \tag{40}$$
$$\theta_2(\mu) = (a_1\mu - 1)(\mu - 1) \tag{41}$$

The constant parameters appearing in these equations are given in Table 1.

A comparison between the semi-infinite strip problem results and the ones predicted from the aforementioned equations can be seen in Fig. 3.

Derivative matrix The derivative matrix, $\bar{\boldsymbol{F}}_{ny}$ of the normalized displacements due to the self equilibrating stresses, $\boldsymbol{u}_y$ with respect to the normalized load parameters, $\boldsymbol{r}_\mathrm{y}$ is:

$$\bar{\boldsymbol{F}}_{ny} = \frac{\partial \boldsymbol{u}_y}{\partial \boldsymbol{r}_\mathrm{y}} = \frac{1}{E}\begin{bmatrix} \sigma_y \dfrac{\partial \delta_\sigma}{\partial c} + t\dfrac{\partial \delta_\tau}{\partial c} & \sigma_y \dfrac{\partial \delta_\sigma}{\partial \mu} + t\dfrac{\partial \delta_\tau}{\partial \mu} & \delta_\tau \\ \sigma_y \dfrac{\partial \theta_\sigma}{\partial c} + t\dfrac{\partial \theta_\tau}{\partial c} & \sigma_y \dfrac{\partial \theta_\sigma}{\partial \mu} + t\dfrac{\partial \theta_\tau}{\partial \mu} & \theta_\tau \end{bmatrix} \tag{42}$$

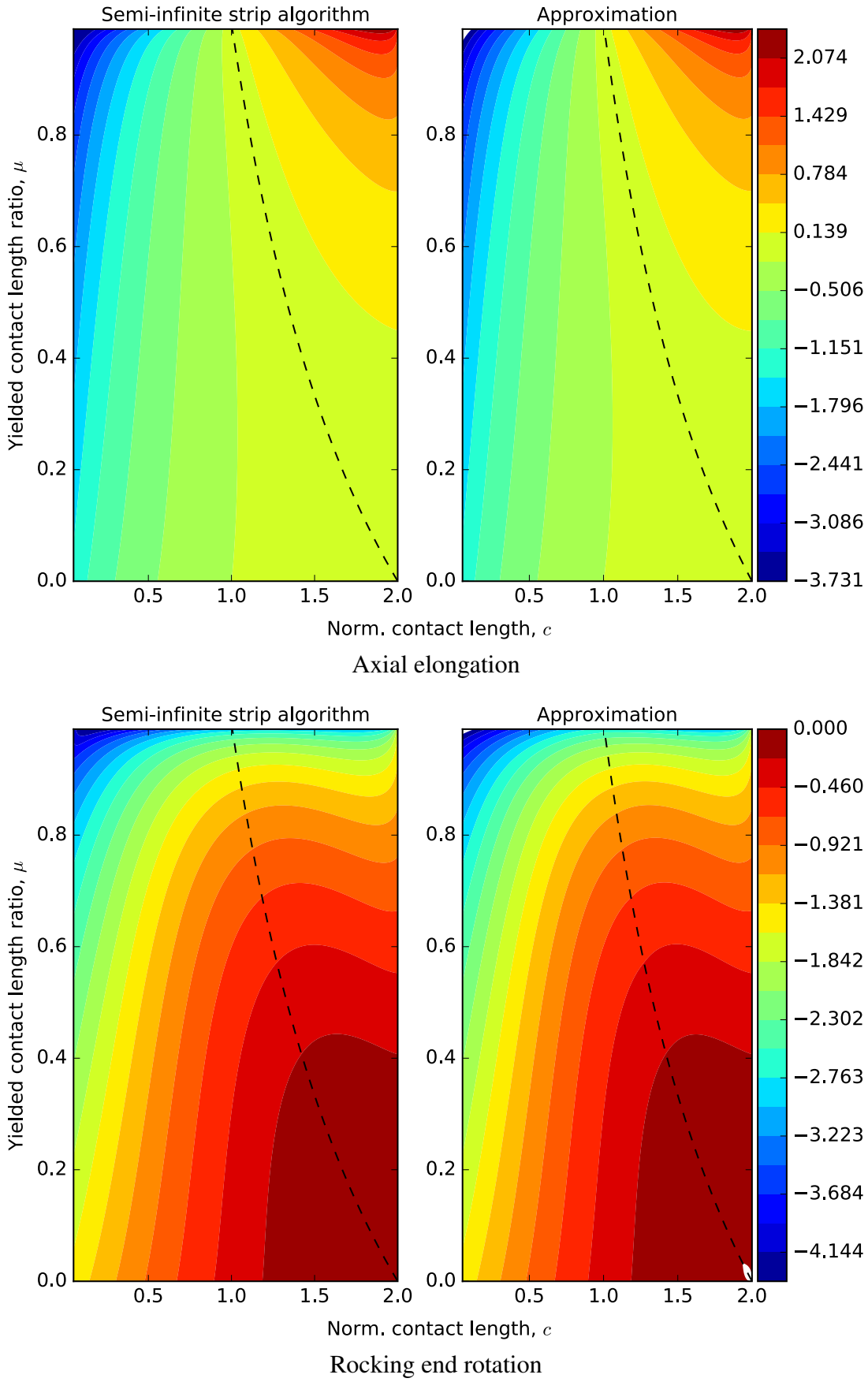

Figure 2: Normalized axial elongation and rocking end rotation for $\sigma_y = 1$.

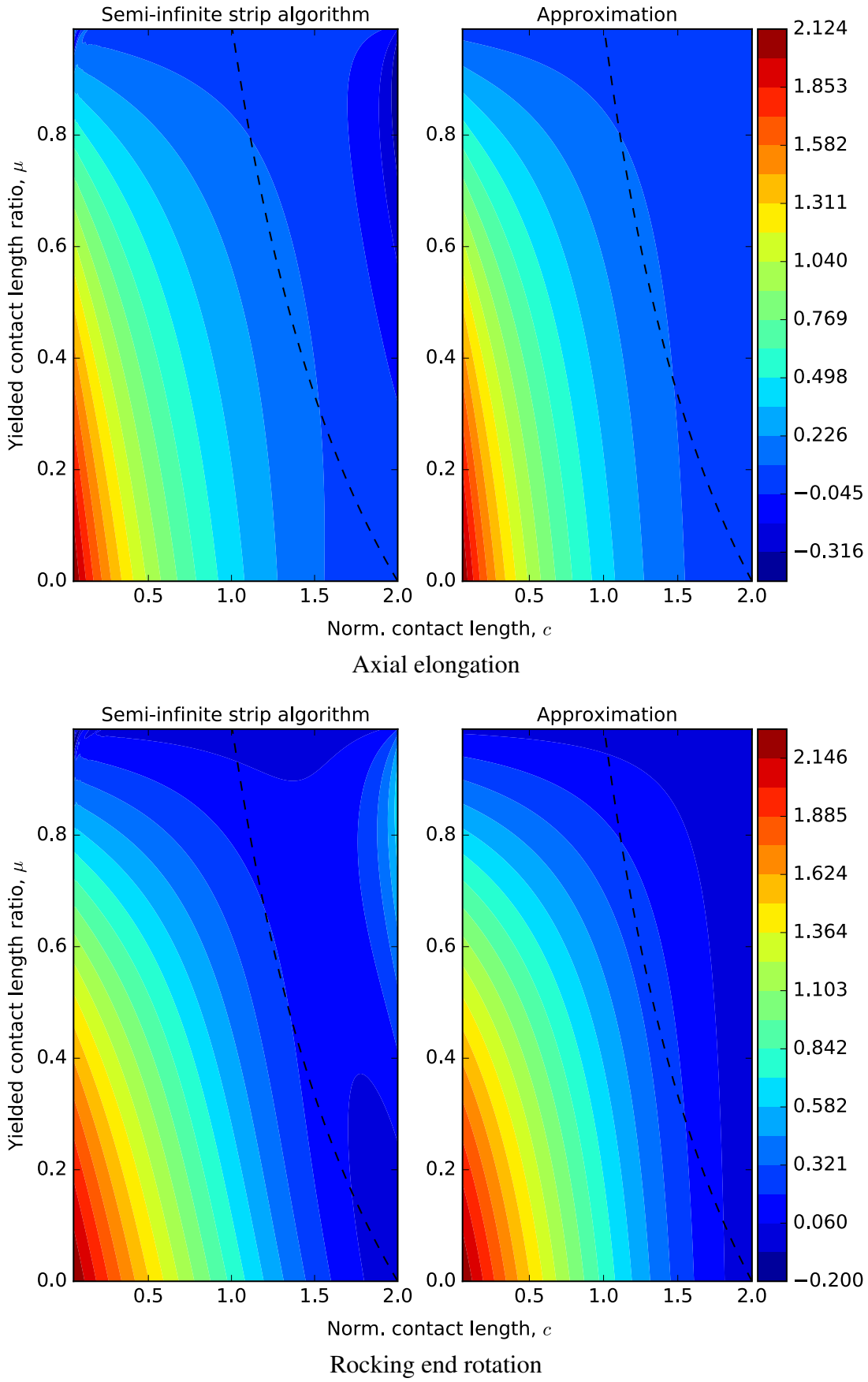

Figure 3: Normalized axial elongation and rocking end rotation for $t = 1$. The approximation is accurate enough for $c \leq 2/(\mu + 1)$.

Changes in the macroelement algorithm due to yielding After the calculation of the rocking interface forces, $\bar{\boldsymbol{Q}}_{\mathrm{r}}$, the yielding condition of Eq. 20 is checked. If the material has yielded, then the following changes are performed in the original algorithm:

- The load parameter vector, $\boldsymbol{r}$ of Eq. 3 is substituted with $\boldsymbol{r}_y$ of Eq. 17
- The corresponding derivative matrix, $\boldsymbol{S}_2$ of Eq. 10 is substituted with $\boldsymbol{S}_{2y}$ of Eq. 19
- The normalized displacement vector due to the self-equilibrating stresses, $\boldsymbol{u}$, (Eq. 4) is substituted with $\boldsymbol{u}_y$ of Eq. 21
- The corresponding derivative matrix, $\bar{\boldsymbol{F}}_n$ of Eq. 11 is substituted with $\bar{\boldsymbol{F}}_{ny}$ of Eq. 42

The rest of the algorithm steps remain the same as in the original elastic material algorithm.

5 EXAMPLES

5.1 Rocking body with constant vertical force with varying yield stress

In this example, a simple rocking body is examined, with height $H = 4$ m, width $B = 1$ m and depth $W = 1$ m and Young's modulus $E = 30$ GPa. The body is loaded on its top central node with a constant vertical force, $N = -2500$ kN (Fig. 4a).

Fig. 4b shows the pushover capacity curves (horizontal force versus horizontal displacement) of this body for varying yield stress values. It can be seen that the maximum strength and the ultimate displacement decrease for decreasing yield stress values.

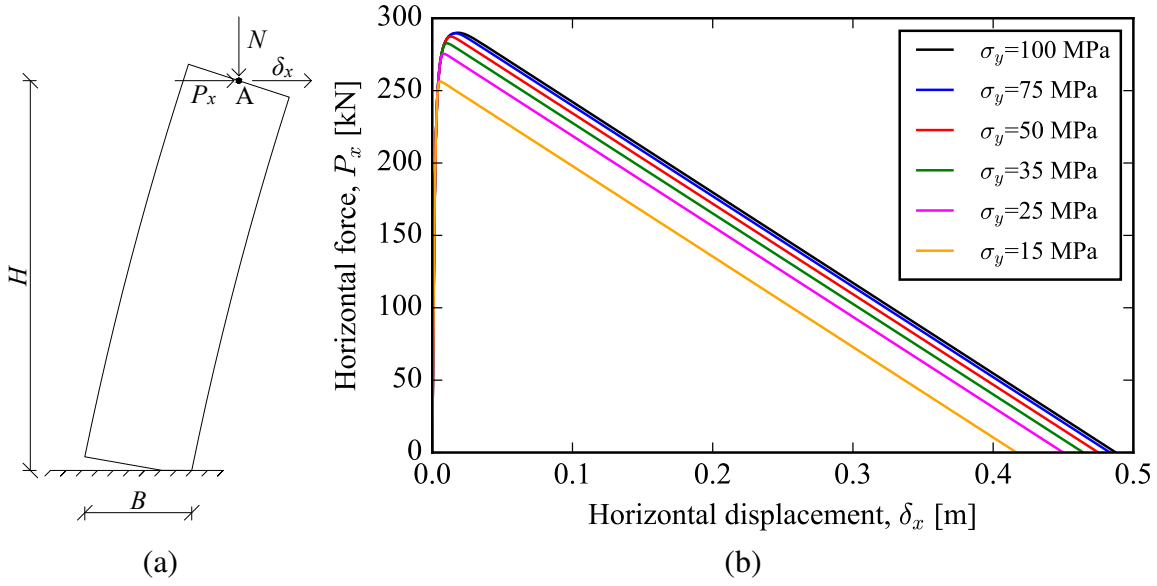

(a) (b)

Figure 4: Rocking body with constant vertical force model and pushover capacity curves for varying stress yield values.

5.2 Comparison of results with Abaqus

In this example, the results produced with the macroelement are compared to those of the commercial software Abaqus [20]. Unfortunately, pushover capacity curves for rocking bodies are very difficult to obtain with Abaqus for a yielding material due to convergence problems.

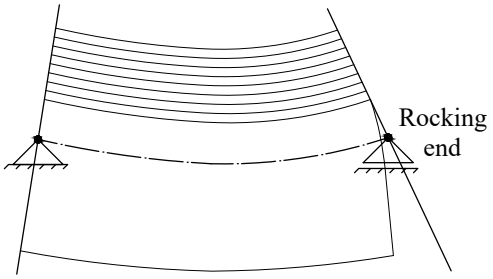

Figure 5: Simply supported beam with rocking end.

For this reason, comparisons are performed for a simply supported beam with a rocking end, which corresponds to the macroelement natural coordinate system (Fig. 5).

The simply supported beam examined has length $L = 8$ m, width $B = 2$ m, depth $W = 1$ m, Young's modulus $E = 30$ GPa, yield stress $\sigma_y = 20$ MPa and is loaded with a constant axial force $N = -1000$ kN.

In Figs. 6a and 6b, the axial elongation and the rocking end rotation are shown for increasing values of the applied moment on the rocking end of the simply supported beam. Fig. 6a refers to the case of a beam with equal applied moments on both its ends, meaning that there is no shear force along the beam, while 6b refers to the case of an applied moment only on the rocking end of the beam, leading to the development of shear forces.

In both cases, it can be seen that the results of the macroelement are very close to the ones obtained using equivalent Abaqus models.

6 CONCLUSION

In this paper, the rocking macroelement formulation previously proposed by the authors, which referred to a member with elastic response, is extended to describe the response of members with yielding material in a monotonic motion. Specific steps of the original formulation are altered to take into account the different stress distributions on the rocking interface, as well as the limited region of the section that remains elastic.

The formulation is applied to solve two example problems. Comparisons of the results with equivalent Abaqus models show very good agreement with the theoretically correct solution.

REFERENCES

[1] R. Skinner, R. Tyler, A. Heine, and W. Robinson, "Hysteretic dampers for the protection of structures from earthquakes," *Bulletin of the New Zealand National Society for Earthquake Engineering*, vol. 13, no. 1, pp. 22–36, 1980.

[2] N. M. Priestley, "Overview of PRESSS research program," *PCI journal*, vol. 36, no. 4, 1991.

[3] S. Sritharan, S. Aaleti, and D. J. Thomas, "Seismic analysis and design of precast concrete jointed wall systems," *ISU-ERI-Ames Report ERI-07404, Submitted to the Precast/Prestressed Concrete Institute*, 2007.

[4] W. Y. Kam, S. Pampanin, A. Palermo, and A. J. Carr, "Self-centering structural systems with combination of hysteretic and viscous energy dissipations," *Earthquake Engineering & Structural Dynamics*, vol. 39, no. 10, pp. 1083–1108, 2010.

[5] G. W. Housner, "The behavior of inverted pendulum structures during earthquakes," *Bulletin of the seismological society of America*, vol. 53, no. 2, pp. 403–417, 1963.

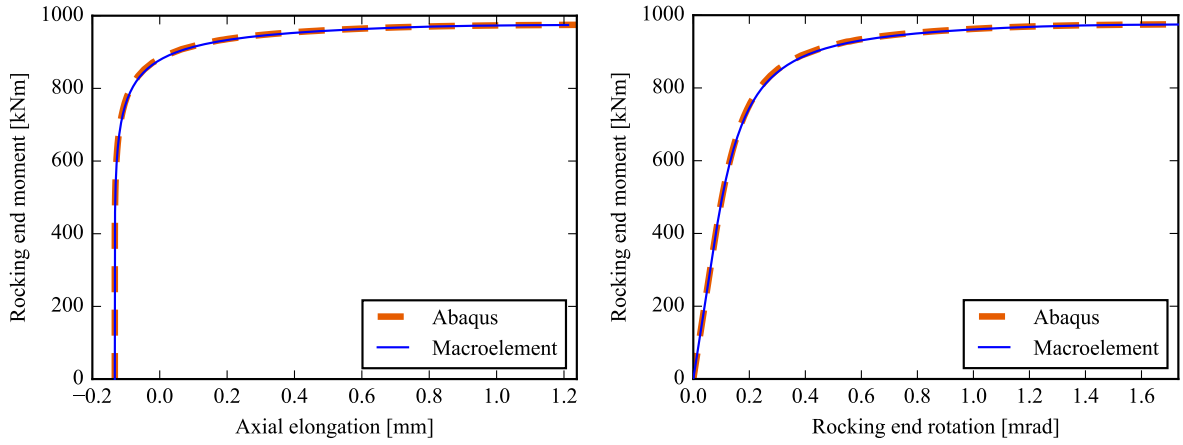

(a)

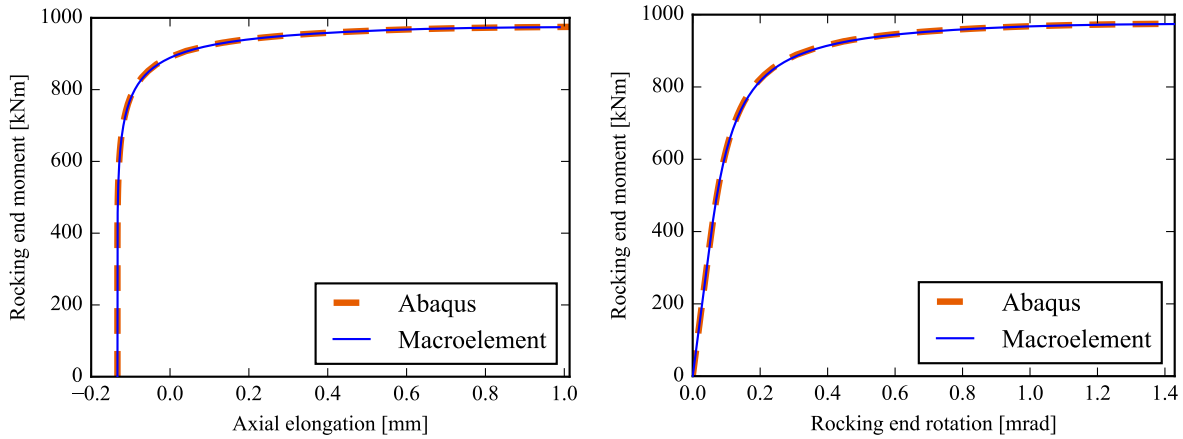

(b)

Figure 6: Axial elongation and rocking end rotation of a rocking simply supported beam and comparison with Abaqus, which is loaded with (a) equal moments on both its ends; (b) a moment only on its rocking end.

[6] C.-S. Yim, A. K. Chopra, and J. Penzien, "Rocking response of rigid blocks to earthquakes," *Earthquake Engineering and Structural Dynamics*, vol. 8, no. 6, pp. 565–587, 1980.

[7] J. Zhang and N. Makris, "Rocking response of free-standing blocks under cycloidal pulses," *Journal of Engineering Mechanics*, vol. 127, no. 5, pp. 473–483, 2001.

[8] E. G. Dimitrakopoulos and M. J. DeJong, "Revisiting the rocking block: closed-form solutions and similarity laws," in *Proceedings of the Royal Society of London A: Mathematical, Physical and Engineering Sciences*, vol. 468, pp. 2294–2318, The Royal Society, 2012.

[9] H. Roh and A. M. Reinhorn, "Analytical modeling of rocking elements," *Engineering Structures*, vol. 31, no. 5, pp. 1179–1189, 2009.

[10] H. Roh and A. M. Reinhorn, "Nonlinear static analysis of structures with rocking columns," *Journal of structural engineering, ASCE*, vol. 136, no. 5, pp. 532–542, 2009.

[11] S. Acikgoz and M. J. DeJong, "The interaction of elasticity and rocking in flexible structures allowed to uplift," *Earthquake Engineering & Structural Dynamics*, vol. 41, no. 15, pp. 2177–2194, 2012.

[12] C. B. Barthes, *Design of Earthquake Resistant Bridges Using Rocking Columns*. PhD thesis, University of California, Berkeley, California, United States, 2012.

[13] A. Belleri, M. Torquati, and P. Riva, "Finite element modeling of rocking walls," in *Proc., 4th ECCOMAS thematic conference COMPDYN*, 2013.

[14] A. Penna, S. Lagomarsino, and A. Galasco, "A nonlinear macroelement model for the seismic analysis of masonry buildings," *Earthquake Engineering & Structural Dynamics*, vol. 43, no. 2, pp. 159–179, 2014.

[15] M. F. Vassiliou, K. R. Mackie, and B. Stojadinović, "Dynamic response analysis of solitary flexible rocking bodies: modeling and behavior under pulse-like ground excitation," *Earthquake Engineering & Structural Dynamics*, vol. 43, no. 10, pp. 1463–1481, 2014.

[16] M. F. Vassiliou, R. Truniger, and B. Stojadinović, "An analytical model of a deformable cantilever structure rocking on a rigid surface: development and verification," *Earthquake Engineering & Structural Dynamics*, 2015.

[17] M. F. Vassiliou, K. R. Mackie, and B. Stojadinović, "A finite element model for seismic response analysis of deformable rocking frames," *Earthquake Engineering & Structural Dynamics*, 2016.

[18] E. Avgenakis and I. N. Psycharis, "Modeling of rocking elastic flexible bodies under static loading considering the nonlinear stress distribution at their base," *Journal of Structural Engineering, ASCE*, 2017.

[19] F. Gaydon and W. Shepherd, "Generalized plane stress in a semi-infinite strip under arbitrary endload," in *Proceedings of the Royal Society of London A: Mathematical, Physical and Engineering Sciences*, vol. 281, pp. 184–206, The Royal Society, 1964.

[20] Dassault Systemes, Providence, Rhode Island, United States, *Abaqus/CAE: User's Manual (6.11)*, 2011.